THE JOURNAL OF BIOLOGICAL CHEMISTRY VOL. 282, NO. 49, pp. 35695–35702, December 7, 2007

Substrate-linked Conformational Change in the Periplasmic Component of a Cu(I)/Ag(I) Efflux System*[S]

Received for publication, May 14, 2007, and in revised form, September 20, 2007 Published, JBC Papers in Press, September 24, 2007, DOI 10.1074/jbc.M703937200

Ireena Bagai[‡], Wenbo Liu[‡], Christopher Rensing[§], Ninian J. Blackburn[¶], and Megan M. McEvoy[‡1]

From the [‡]Department of Biochemistry and Molecular Biophysics and [§]Department of Soil, Water, and Environmental Science, University of Arizona, Tucson, Arizona 85721 and the [¶]Department of Environmental and Biomolecular Systems, Oregon Graduate Institute School of Science and Engineering, Oregon Health and Science University, Beaverton, Oregon 97006-8921

Gram-negative bacteria utilize dual membrane resistance nodulation division-type efflux systems to export a variety of substrates. These systems contain an essential periplasmic component that is important for assembly of the protein complex. We show here that the periplasmic protein CusB from the Cus copper/silver efflux system has a critical role in Cu(I) and Ag(I) binding. Isothermal titration calorimetry experiments demonstrate that one Ag(I) ion is bound per CusB molecule with high affinity. X-ray absorption spectroscopy data indicate that the metal environment is an all-sulfur 3-coordinate environment. Candidates for the metal-coordinating residues were identified from sequence analysis, which showed four conserved methionine residues. Mutations of three of these methionine residues to isoleucine resulted in significant effects on CusB metal binding *in vitro*. Cells containing these CusB variants also show a decrease in their ability to grow on copper-containing plates, indicating an important functional role for metal binding by CusB. Gel filtration chromatography demonstrates that upon binding metal, CusB undergoes a conformational change to a more compact structure. Based on these structural and functional effects of metal binding, we propose that the periplasmic component of resistance nodulation division-type efflux systems plays an active role in export through substrate-linked conformational changes.

Efflux systems of the resistance nodulation division (RND)[2] family are key players in the intrinsic and acquired antibiotic resistance of Gram-negative bacteria (1). These systems confer resistance to otherwise lethal concentrations of drugs and metal ions, and they also mediate efflux of bacterial products such as siderophores, peptides, and quorum-sensing signals (2, 3). With antibiotic-resistant pathogens representing a growing threat to human health, understanding these efflux systems is of significant importance.

RND-type efflux systems form a transenvelope complex comprised of three fundamental components: an energy-utilizing inner membrane protein (4), an outer membrane factor, and a periplasmic component (5). The inner membrane components are proton-substrate antiporters of the RND protein superfamily, which are subclassified on the basis of their exported substrate (4). Members of the heavy metal efflux subfamily of RND transport systems are highly substrate-specific, with the ability to differentiate between monovalent and divalent ions (4). In contrast, the hydrophobe/amphiphile efflux (HAE) subfamily of RND protein systems has significantly broader substrate recognition. Members of the HAE-RND systems transport a wide range of structurally unrelated molecules, including antibiotics, dyes, detergents, bile salts, organic solvents, and antimicrobial peptides (6).

Insights into the functions of the three fundamental components of RND efflux systems have been gathered from studies of a variety of RND systems. By far, the most information at the structural and biochemical levels is known for the inner and outer membrane proteins. The overall picture that has emerged is that the inner and outer membrane proteins form a channel that spans the periplasmic space (7, 8). The substrate is taken up from either the inner membrane, cytoplasm, or periplasm, depending on the properties of the substrate and the particular efflux system (9). The RND protein drives substrate export through the channel formed by the outer membrane protein utilizing the proton gradient across the inner membrane. Although the periplasmic component is an essential part of RND efflux systems (10), the role it plays in the efflux process is much less clear.

Several functions have been postulated for the periplasmic component. It is often termed an adaptor protein, which may have a function in bridging the inner and outer membrane components. This role is supported by biochemical experiments that have shown a direct interaction between this component and the inner and outer membrane proteins (7). More recent studies suggest that the periplasmic component could contribute to the regulation of the open and closed states of the outer membrane protein. Evidence for this function of the periplasmic adaptor protein is given by the observation of conformational variants in the crystal structure of the periplasmic protein AcrA from the AcrAB-TolC HAE-RND efflux system (11) and observation of direct interactions between the coiled regions of the periplasmic protein and outer membrane protein

* This work was supported by National Institutes of Health Grants GM54803 (to N. J. B.) and GM079192 (to M. M. M.). The costs of publication of this article were defrayed in part by the payment of page charges. This article must therefore be hereby marked "*advertisement*" in accordance with 18 U.S.C. Section 1734 solely to indicate this fact.

[S] The on-line version of this article (available at http://www.jbc.org) contains supplemental Fig. S1.

[1] To whom correspondence should be addressed: 1041 E. Lowell St., Dept. of Biochemistry and Molecular Biophysics, University of Arizona, Tucson, AZ 85721. Fax: 520-621-1697; E-mail: mcevoy@email.arizona.edu.

[2] The abbreviations used are: RND, resistance, nodulation, division; ITC, isothermal titration calorimetry; EXAFS, extended x-ray absorption fine structure; CHAPS, 3-[(3-cholamidopropyl)dimethylammonio]-1-propanesulfonate; MOPS, 3-(*N*-morpholino)propanesulfonic acid; HAE, hydrophobe/amphiphile efflux; AHT, anhydrotetracycline; DW, Debye Waller.

(12). However, the periplasmic protein likely has a further functional role, because even a constitutively open mutant of an outer membrane protein requires the periplasmic component (13). In a reconstituted system without the outer membrane protein, the periplasmic adaptor AcrA is essential to the function of the RND pump AcrD (14), which further supports the hypothesis that the periplasmic proteins can play an active role in substrate capture and extrusion.

CusCFBA, the Cu(I) and Ag(I) efflux system from *Escherichia coli*, consists of CusB, the periplasmic protein, CusA, the inner membrane proton/substrate antiporter of the heavy metal efflux-RND family, and CusC, the outer membrane protein (10, 15, 16). In addition to the three fundamental proteins, the Cus system has a fourth component, the small periplasmic metal-binding protein CusF, which has homologs only in putative monovalent metal ion resistance systems (10). In addition to conferring Ag(I) resistance (15), the CusCFBA system has been shown to be important for copper resistance primarily under anaerobic conditions, suggesting that its other physiologically relevant substrate is Cu(I) (17). Copper and silver belong to the same group of the periodic table; therefore, Cu(I) and Ag(I) have similar coordination chemistries and can be treated interchangeably in many cases (18). However, silver is predominantly found in the Ag(I) oxidation state under both aerobic and anaerobic conditions, whereas Cu(I) only predominates under anaerobic conditions. To address the role of the periplasmic component, we examined CusB from the CusCFBA system as a representative of the periplasmic proteins of RND efflux systems.

EXPERIMENTAL PROCEDURES

Protein Expression and Purification—Genomic DNA from *E. coli* strain W3110 was used to amplify the *cusB* gene. The primers used for the PCR contained unique restriction sites at the 5′ end (EcoRI) and 3′ end (XhoI). After restriction enzyme digestion of the PCR product, it was ligated into the pASK-IBA3 (IBA GmbH, Göttingen, Germany) vector. The result was a construct that contained the full-length *cusB* gene followed by region encoding a short cloning artifact (LEVDLQGDHGL) and a C-terminal Strep affinity tag (SAWSHPQFEK).

The *cusB*-containing plasmid was transformed into *E. coli* BL21-(DE3). Cells were grown in LB media containing 100 μg/ml ampicillin at 37 °C until they reached an A_{600} of 0.6–1.0, then induced with 200 μg/liter of anhydrotetracycline (AHT), and grown at 30 °C for another 6–8 h. Cells were harvested by centrifugation and frozen at −20 °C.

Cell pellets were resuspended in 50 ml of 100 mM Tris (pH 8.0), 150 mM NaCl per liter of cell culture. Protease inhibitors (leupeptin (final concentration 2 μg/ml), pepstatin (final concentration 2 μg/ml), and phenylmethylsulfonyl fluoride (final concentration 0.5 mM)) and DNase I (~150 units)) were added, and then cells were lysed by a French press. CHAPS (0.1% w/v) (MP Biomedicals) was added to the lysate, and cells were then pelleted by centrifugation at 31,000 × *g*. The supernatant was loaded onto *Strep*-Tactin-resin (IBA GmbH) affinity column. After washing the column with 100 mM Tris (pH 8.0), 150 mM NaCl buffer, protein was eluted using the same buffer, plus 2.5 mM desthiobiotin. The fractions were dialyzed *versus* 50 mM Tris (pH 9.0) buffer and loaded onto a Mono Q 10/100 GL anion exchange column (Amersham Biosciences) equilibrated with the same buffer. CusB was eluted from the column by a linear gradient of 0–300 mM NaCl in 50 mM Tris (pH 9.0). Aliquots of the fractions were run on SDS-polyacrylamide gels and stained with Coomassie to determine purity. CusB protein was also verified by Western blot analysis using horseradish peroxidase-conjugated antibody specific to the *Strep* tag (IBA GmbH). The N-terminal sequence of CusB was confirmed by sequencing. Fractions >95% pure were pooled and dialyzed in appropriate buffer and concentrated using Amicon concentrators with a 5-kDa molecular weight cut-off. Protein concentrations were determined using the BCA assay (Pierce) for all the experiments except EXAFS for which the Bradford assay (19) (Bio-Rad) was used.

Isothermal Titration Calorimetry—ITC measurements were performed on a Microcal VP-ITC microcalorimeter (Northampton, MA), typically at 25 °C. The titrant solution was made by mixing appropriate amounts of stock metal solution (90 mM $AgNO_3$ in nanopure Milli-Q water) with buffer retained from the final dialysis of the protein sample. CusB was extensively dialyzed in 50 mM cacodylate (pH 7.0). Both protein and titrant were thoroughly degassed in a ThermoVac apparatus (Microcal). For a titration experiment, ~1.7 ml of 22 μM CusB was placed in a reaction cell and injected over 20 s with 10 μl of 300 μM $AgNO_3$ solution with a 5-min interval between each injection. The titrations of the CusB mutants M21I, M36I, M38I, and M283I were carried out as described for wild-type CusB, using protein concentrations of 18.0, 19.0, 20.0, and 24.7 μM, respectively. To ensure adequate mixing of the titrand and the titrant, the reaction cell was continuously stirred at 300 rpm. A total of 25 injections was made. The heat because of dilution, mechanical effects, and other nonspecific effects were accounted for by averaging the last three points of titration and subtracting that value from all data points (20, 21). Data were fitted using a single-site binding model in the Origin software package (MicroCal). The software uses a nonlinear least squares algorithm and the concentrations of the titrant and the titrand to fit the enthalpy change per injection to an equilibrium binding equation. The binding enthalpy change ΔH, association constant K_a, and the binding stoichiometry n were permitted to float during the least squares minimization process and taken as the best fit values.

X-ray Absorption Spectroscopy—Samples for EXAFS were prepared in an anaerobic chamber. CusB was first dialyzed in 20 mM MOPS (pH 7.0). Ascorbate solution buffered at pH 7.0 was then added to argon-purged protein at a final concentration of 50 mM. $CuCl_2$ was added such that the ratio of CusB to Cu(I) was 1:1. The protein was further dialyzed against 20 mM MOPS, 10 mM ascorbate (pH 7.0), to remove unbound copper. The final concentration of protein was determined using the Bradford assay (19). 80 μl of CusB-Cu(I) was mixed with 20 μl of ethylene glycol, transferred to EXAFS vials, and then flash-frozen in liquid nitrogen.

Collection and Analysis of XAS Data—CuK-edge (8.9 keV) EXAFS and x-ray absorption near edge structure data were collected at the Stanford Synchrotron Radiation Laboratory operating at 3 GeV with currents between 100 and 50 mA. All sam-

ples were measured on beam line 9-3 using a Si(220) monochromator and a rhodium-coated mirror upstream of the monochromator with a 13 keV energy cutoff to reject harmonics. A second rhodium mirror downstream of the monochromator was used to focus the beam. Data were collected in fluorescence mode using a high count rate Canberra 30-element germanium array detector with maximum count rates below 120 kHz. A 6-μ Z-1 nickel oxide filter and Soller slit assembly were placed in front of the detector to reduce the elastic scatter peak. Six scans of a sample containing only sample buffer were collected, averaged, and subtracted from the averaged data for the protein samples to remove Z-1 K_β fluorescence and produce a flat pre-edge base line. The samples (80 μl) were measured as aqueous glasses (>20% ethylene glycol) at 10 K. Energy calibration was achieved by reference to the first inflection point of a copper foil (8980.3 eV) placed between the second and third ionization chamber. Data reduction and background subtraction were performed using the program modules of EXAFSPAK (22). Data from each detector channel were inspected for glitches or dropouts before inclusion in the final average. Spectral simulation was carried out using the program EXCURVE 9.2 (23–26) as described previously (27).

Site-directed Mutagenesis and Growth Inhibition Studies of CusB—The QuikChange site-directed mutagenesis protocol (Stratagene, La Jolla, CA) was used to alter the individual methionines to isoleucines in CusB. Plasmid pASK3 containing the *cusB* gene was used as a template. Primer pairs used to introduce the point mutations were antiparallel and overlapping. PCR products were treated with DpnI to digest the *dam*-methylated template plasmid. The correct mutations were verified by DNA sequence analysis. The purified PCR product containing the point mutation was transformed into EC950 (Δ*cueO* Δ*cusB*) strain (10) of *E. coli*. Wild-type *cusB* and an empty pASK3 vector (without the *cusB* gene) were also transformed into EC950 to use as controls in the growth inhibition studies.

For growth inhibition experiments, mutants, wild type, and the cells containing empty vector were grown overnight in LB medium. Cells were diluted 1:100 in fresh media and grown at 37 °C until they reached an A_{600} of ~0.5. At this point, the cells were subjected to two different protocols. For one set, cells were induced for CusB expression at the same time as they were exposed to copper by streaking the cells directly on LB agar plates containing 100 μg/ml ampicillin, 50 μg/liter AHT, and varying concentrations of $CuCl_2$ (0.0, 0.5, 0.75, 1.0, and 1.5 mM). For the second set, the cells were induced to express CusB before subjecting them to metal stress. The cells at an A_{600} of 0.5 were induced with 50 μg/liter AHT and grown at 30 °C until they reached an A_{600} of ~1.0. At this point, cells were streaked on LB agar plates containing 100 μg/ml ampicillin and varying concentrations of $CuCl_2$ (0.0, 0.5, 1.0, 1.25 and 1.5 mM) but no AHT. All plates were incubated at 30 °C for ~18 h.

Analytical Ultracentrifugation—Sedimentation equilibrium analysis was performed in a Beckman Optima XL-1 analytical ultracentrifuge using an An-60Ti rotor and an absorbance optical system. A six-channel equilibrium centerpiece equipped with sapphire windows was used to run three sample-solvent pairs simultaneously. Sample and solvent volumes were 110 and 125 μl, respectively. Data were collected at 4 °C at speeds of 15,000, 20,000, and 25,000 rpm on samples at three concentrations ranging from 5 to14 μM for apo-CusB and 5 to 14 μM CusB with 10–28 μM $AgNO_3$ for CusB-Ag(I). Samples were allowed to equilibrate for 12 h at each speed, after which five replicate scans were taken every 4 h in a step size of 0.005 cm. These scans, spaced 4 h apart, were overlaid to determine whether equilibrium had been established. Final equilibrium scans were then performed in a step size of 0.001 cm, and absorbance was monitored at 280 and 255 nm. Fifteen replicate scans were taken and averaged at every radial increment.

The SEDNTERP program (28) was used to calculate the partial specific volume (0.7318 ml/g) and the buffer density (1.00605 g/ml) at 4 °C. The base-line offset was constrained to ~0.04 for all the data sets. The distribution of single ideal species and monomer-dimer/monomer-trimer equilibrium species was analyzed according to equations described by McRorie and Voelker (29). All fits were done by nonlinear least square analysis of the primary data using the general curve fit function of Kaleidagraph version 3.51 (Synergy Software).

Size Exclusion Chromatography—Size exclusion chromatography was performed using a Superdex 200 10/300GL analytical column (Amersham Biosciences) on an Akta Prime System (Amersham Biosciences). 60–70 μl of protein at a concentration of 180 μM was loaded onto the column pre-equilibrated with 50 mM sodium phosphate (pH 7.0). The column was run at a flow rate of 0.4 ml/min, and absorbance was measured at 280 nm. Fractions of 500 μl were collected. For Ag(I)-CusB, $AgNO_3$ dissolved in water was added to the protein at a 2-fold molar excess. The size exclusion column was calibrated with the following globular protein markers (molecular mass and retention volumes are reported): thyroglobulin (669 kDa, 9.7 ml), ferritin (440 kDa, 11.2 ml), catalase (232 kDa, 13.0 ml), aldolase (158 kDa, 13.5 ml), albumin (67 kDa, 14.4 ml), ovalbumin (43 kDa, 15.3 ml), chymotrypsinogen A (25 kDa, 17.1 ml), and ribonuclease (13.7 kDa, 17.7 ml).

RESULTS

To investigate whether CusB could play a role in substrate binding, we employed isothermal titration calorimetry (ITC) to study the binding of Ag(I) by CusB *in vitro*. ITC detects changes in the heat absorbed or released during a binding event (*i.e.* the binding enthalpy change). The titration of Ag(I) into the solution of apo-CusB showed a change in binding enthalpy that was not seen in the control titrations without CusB protein, clearly indicating a binding event (Fig. 1). The large exothermic peaks eventually diminished into just the heat of dilution after ~11 injections. A single-site binding model was used to fit the data, yielding a K_a value of 4.04×10^7 M^{-1} (corresponding to a K_d of 24.7 nM) and a stoichiometry of Ag(I) to CusB of 0.72 ± 0.01. The dissociation constant should be treated as an approximate value as it is at the lower limits of measurement by ITC. This affinity is similar to that measured for the periplasmic copper- and silver-binding protein CusF from the Cus system (21), and it clearly demonstrates that CusB is a metal-binding protein.

To identify the potential metal ligands in CusB, we performed x-ray absorption spectroscopy of CusB bound to Cu(I). X-ray absorption spectroscopy data were collected on two independent samples of copper-loaded CusB and gave identical

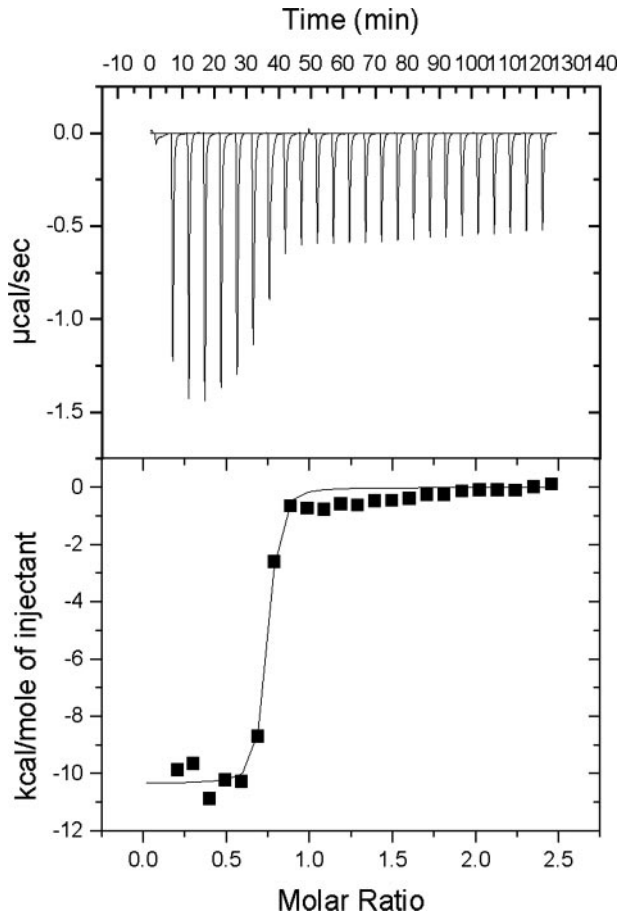

FIGURE 1. **ITC data for titration of 22 μM CusB with 300 μM $AgNO_3$ at 25 °C.** Both solutions were made in 50 mM cacodylate (pH 7.0). *Top*, raw data. *Bottom*, plot of integrated heats *versus* Ag(I)/CusB ratio. The *solid line* represents the best fit for a one-site binding model.

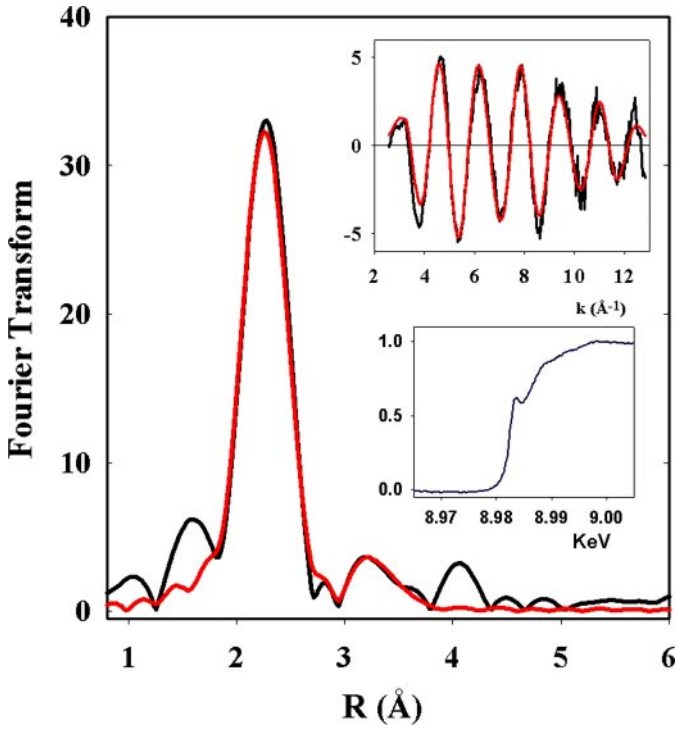

FIGURE 2. **EXAFS data for CusB-Cu(I).** Experimental (*black*) and simulated (*red*) Fourier transforms and EXAFS (*top inset*) for CusB-Cu(I). X-ray absorption edge intensity of 8983 eV is diagnostic of 3-coordinate geometry (*bottom inset*).

results within experimental error. The absorption edge region of the spectrum (Fig. 2, *inset*) shows a weak feature at 8983.7 eV with intensity equal to 0.62 of the normalized edge height. The position and intensity of this peak is characteristic of Cu(I) bound to the protein, in a 3-coordinate environment (30, 31). Fig. 2 shows the Fourier transform and extended x-ray absorption fine structure (EXAFS) for a representative sample. The spectrum consists of intense oscillations extending beyond $k = 12.8$ Å^{-1}, the energy cutoff used to avoid background errors because of small amounts of contaminating zinc in the sample. The first shell of the phase-corrected Fourier transform maximizes at ~2.3 Å (characteristic of Cu(I)-thioether or thiolate coordination). The best fits to the data were obtained with three Cu-S scattering interactions with Cu-S bond length of 2.287 Å and a Debye Waller factor (DW, $2\sigma^2$) of 0.011 Å^2 ($F = 0.43$). We also tested fits that utilized two and four Cu-S interactions. These gave similar Cu-S bond lengths but had uniformly worse F values (0.70 and 0.56, respectively). Because the simulated bond lengths remained close to those expected for 3-coordination, this analysis confirmed the 3-coordinate assignment. A fit using two Cu-S and one Cu-O/N interaction had a more acceptable F value (0.51), with two Cu-S at 2.300 Å ($2\sigma^2 = 0.006$ Å^2) and Cu-O/N at 2.050 Å ($2\sigma^2 = 0.017$ Å^2), but the large DW term for the single low-Z copper scatterer suggested this latter model was less reasonable than the three Cu-S fits. However, the 3 sulfur fit also has a high DW for the Cu-S shell suggesting some heterogeneity in the Cu-S distances. Splitting these distances did not lead to improvements in the F value. We conclude that the most reasonable model to fit the data is three slightly differing Cu-S interactions at an average distance of 2.29 Å from the central Cu(I) atom.

Because CusB does not contain any cysteine residues, the sulfur-containing species in CusB that coordinate Cu(I) are methionine residues. The unusually long Cu-S bond length of 2.29 Å is in agreement with this conclusion, because 3-coordinate Cu-cysteinate ligated sites typically exhibit Cu-S bond lengths in the 2.23–2.28-Å range (30, 31). Here the weaker donor properties of the thioether ligand appear to lead to lengthening of the Cu-S(Met) bonds. Methionines are commonly used in periplasmic proteins for metal coordination because the oxidizing environment of the periplasm renders cysteine less effective. However, few good models exist for 3-coordinate methionine-coordinated Cu(I), and the CusB site represents the first such structure to be described for a metalloprotein.

To identify candidates for the three metal-coordinating methionines detected from the EXAFS data, the conservation of the methionines in CusB was examined. From a BLAST search with the mature CusB sequence, the top 51 sequences (considering only one sequence from each genus) were selected for alignment. The alignment, generated with ClustalW using the default parameters, shows that of the nine methionines in the mature sequence of CusB, four methionines (Met-21, Met-36, Met-38, and Met-283) are well conserved in these proteins (supplemental Fig. 1). Methionine is always found at position

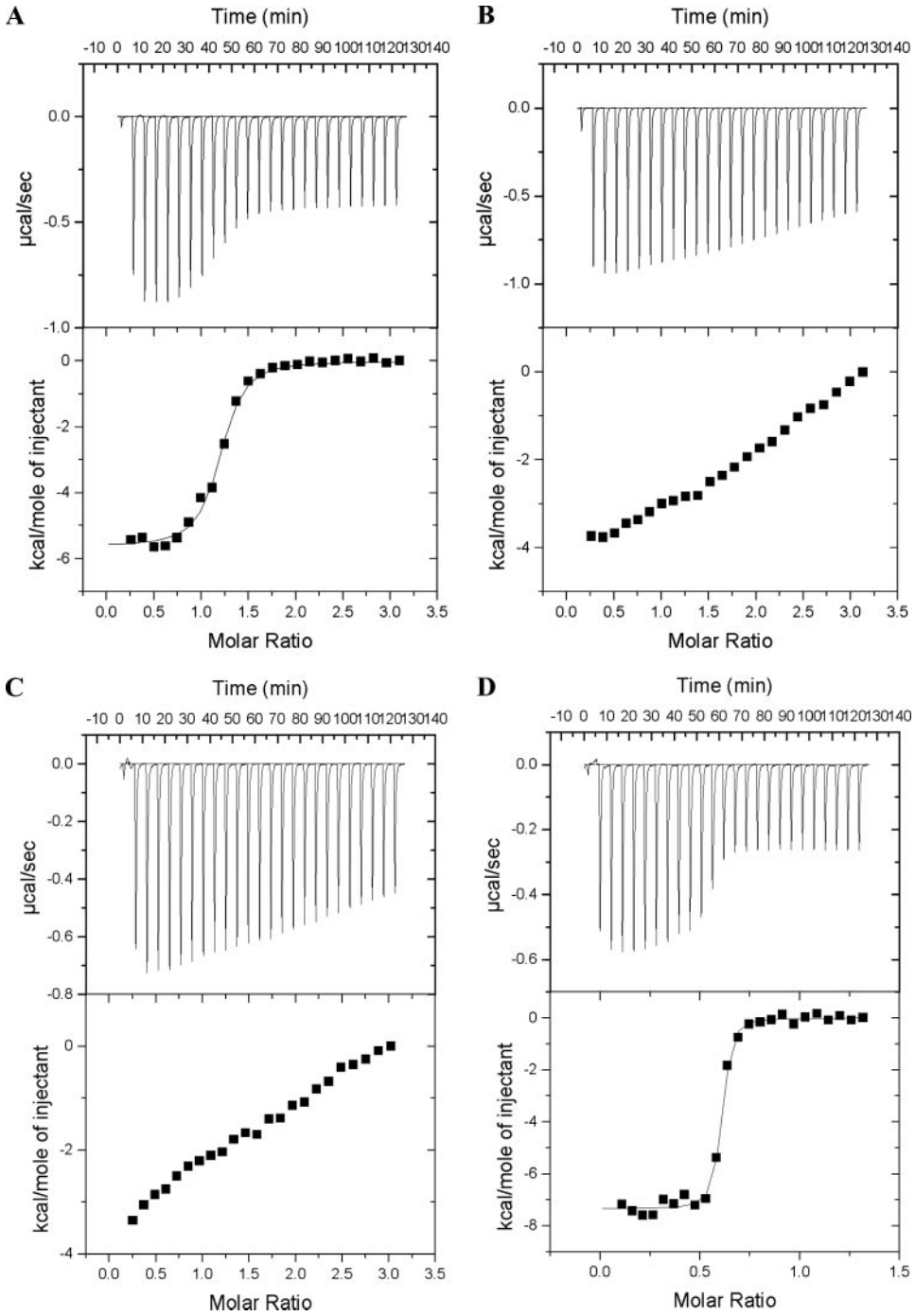

FIGURE 3. **ITC data for titration of CusB variants with $AgNO_3$.** Experimental conditions were similar to those described for wild-type CusB. *Top*, raw data. *Bottom*, plot of integrated heats *versus* Ag(I)/CusB ratio. The *solid line* represents the best fit for a one-site binding model. *A,* CusB M21I; *B,* CusB M36I; *C,* CusB M38I; and *D,* CusB M283I.

21, with one exception where it is histidine. Position 36 is always a methionine, except for one occurrence where it is an aspartate. Position 38 is always conserved as a methionine. Position 283 is usually found as methionine (47 of 52 sequences) but is also found as a leucine, threonine, or alanine. Furthermore, in more extensive alignments (data not shown) methionines 21, 36, and 38 are primarily conserved in the periplasmic proteins of putative monovalent metal resistance systems, although Met-283 is conserved among periplasmic proteins exporting a variety of substrates. The other methionine positions, 162, 199, 213, 296, and 370, show much greater variability in the homologs and do not consistently have the appropriate properties for metal coordination. These positions are usually occupied by hydrophobic residues. Therefore, of the methionines in CusB, three of the four well conserved methionines are likely candidates for the metal-coordinating methionines.

To identify which three of the four methionines are involved in metal binding, ITC was used to determine the ability of the four individual CusB mutants M21I, M36I, M38I, and M283I to bind Ag(I) *in vitro* (Fig. 3, *A–D*). CusB M21I showed a 10-fold reduction in the binding affinity for Ag(I) as compared with wild-type CusB, with a dissociation constant of 0.2 μM. CusB M36I and M38I showed no specific binding to Ag(I). The affinity of CusB M283I for Ag(I) was the same as wild type, with a dissociation constant of 20 nM. Thus, the most significant effects in metal binding affinity are seen for CusB variants M36I and M38I, with a more modest decrease in affinity seen for CusB M21I.

To test whether metal binding by CusB plays a functional role in metal resistance, we examined the ability of *E. coli* cells containing the individual CusB variants M21I, M36I, M38I, and M283I to survive under elevated concentrations of copper. Cells containing each of the CusB variants were compared with wild-type CusB for their growth ability in copper-rich environments (Table 1), in a background where the chromosomal copies of *cusB* and the multicopper oxidase *cueO* have been deleted. The latter deletion has been shown previously to be required to observe a copper-sensitive phenotype under aerobic conditions (10, 15). Cells were either pre-induced to express CusB before subjecting them to copper stress (set a in Table 1) or were induced for CusB expression at the same time as they were exposed to the copper-containing media (set b in Table 1) as described under "Experimental Procedures." The results obtained from these two sets of experiments are similar. Cells containing wild-type CusB or each of the variants grow normally up to 0.5 mM $CuCl_2$ concen-

TABLE 1

Growth behavior of CusB wild-type and variants on agar plates containing various concentrations of $CuCl_2$

The symbols used are as follows: ++, wild-type growth; +, inhibited growth; ++m, growth with mucoid appearance; +m, inhibited growth with mucoid appearance; 0, no growth; ND, not determined.

Complementing gene in *trans*	$CuCl_2$ (mM)													
	0.0		0.5		0.75		1.0		1.25		1.5		2.0	
	a	b	a	b	a	b	a	b	a	b	a	b	a	b
Wild-type *cusB*	++	++	++	++		++	++	++	+m		+	+	0	0
cusB (M21I)	++	++	++	++		+	+m	0	0		0	0	0	0
cusB (M36I)	++	++	++	++		+	+m	0	0		0	0	0	0
cusB (M38I)	++	++	++	++	ND	++m	+m	0	0	ND	0	0	0	0
cusB (M283I)	++	++	++	++		++m	+m	+m	0		0	0	0	0
No *cusB* (pASK-IBA3)	++	++	++	++		+	0	0	0		0	0	0	0

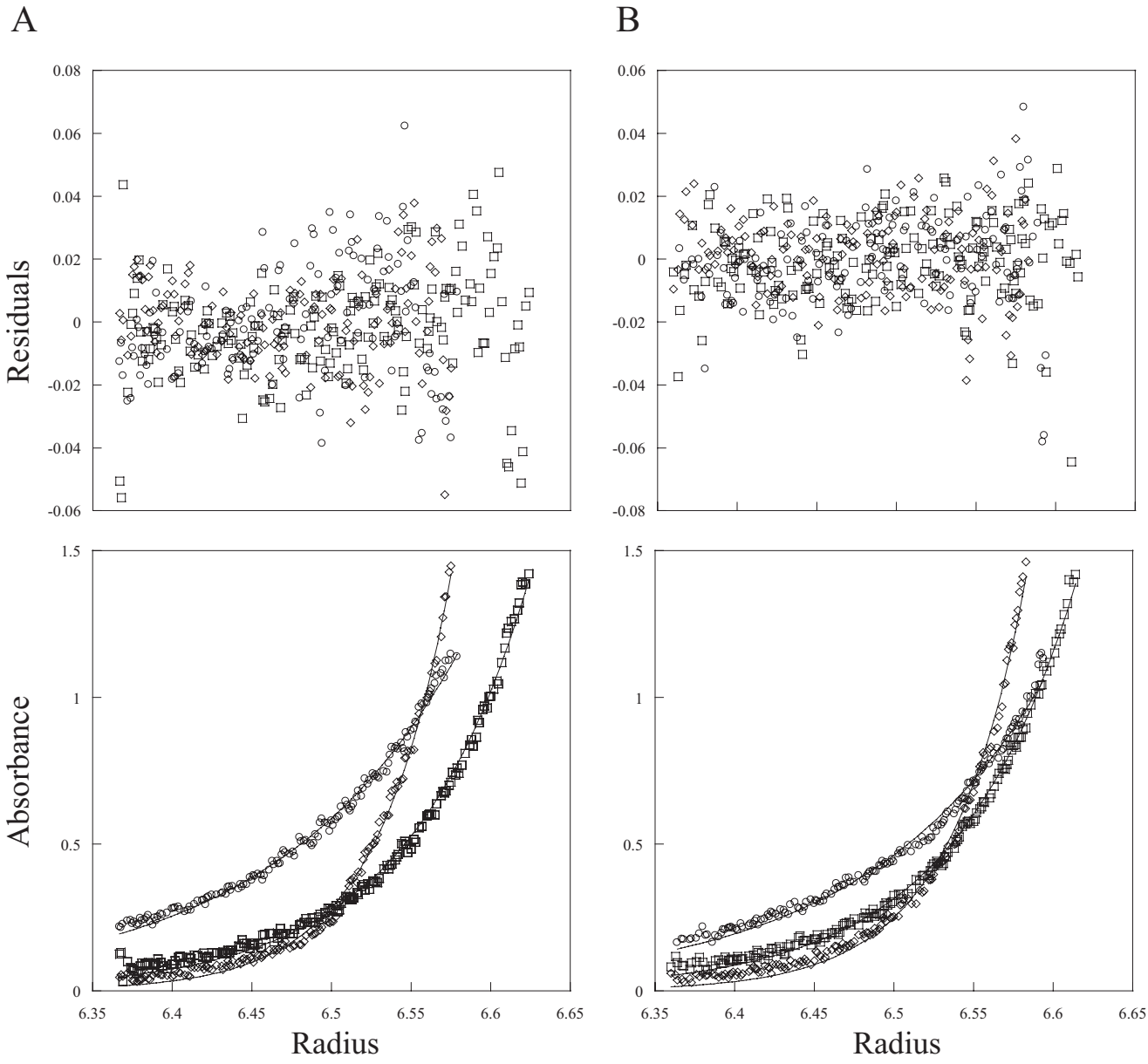

FIGURE 4. **Sedimentation equilibrium analysis of apo-CusB (*A*) and CusB-Ag(I) (*B*).** *Bottom panels* show data points and curve fits for protein at a concentration of ~9 μM (A_{280} = 0.43) at three different speeds of 15,000 (○), 20,000 (□), and 25,000 (◇) rpm with scans at 280 nm. *Top panels* show the residuals left when subtracting the calculated values from the measured points.

tration. When CusB expression was induced before the cells were subjected to metal stress (set a), all the cells expressing CusB variants showed copper sensitivity with mucoid colonies by 1.0 mM $CuCl_2$ concentration. For the cells that were not pre-induced to express CusB (set b), at 1.0 mM $CuCl_2$ the cells with CusB variants M21I, M36I, and M38I did not show

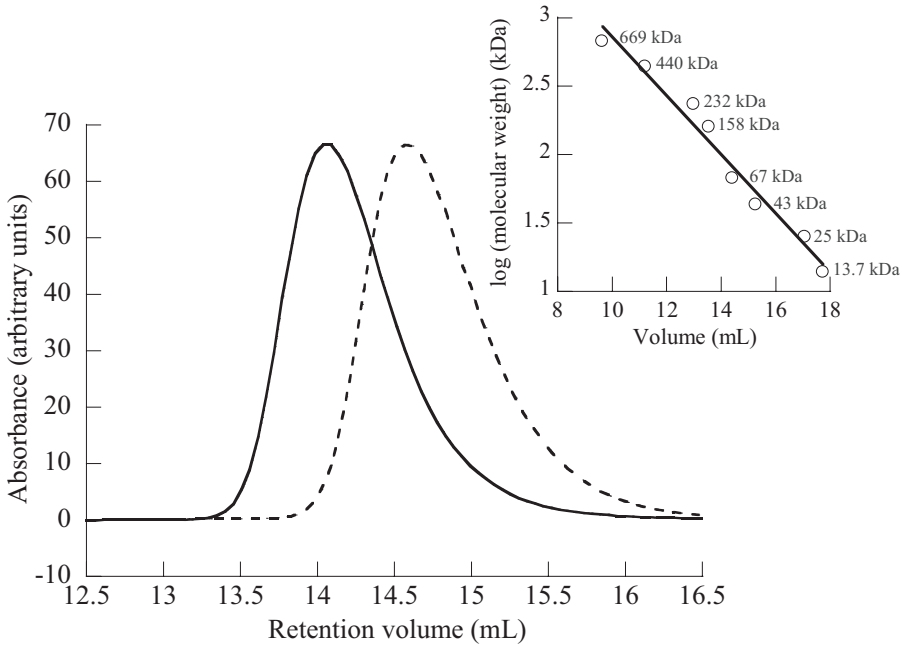

FIGURE 5. **Analytical gel filtration on a Superdex 200 10/300GL analytical column of apo- and Ag(I)-bound CusB in 50 mM sodium phosphate (pH 7.0).** *Solid line* represents the apo-CusB, which eluted at ~14.1 ml, and the *dashed line* represents CusB-Ag(I), which eluted at ~14.6 ml. Absorbance values were normalized. *Inset plot* shows the relative retention volumes of protein molecular weight standards.

growth, cells with the CusB M283I variation showed diminished growth, and the cells with wild-type CusB were not inhibited by these concentrations of copper. Although the mutation of M283 lowered the resistance of cells compared with the wild type, the CusB M283 variant could survive higher copper concentrations compared with the other three variants. The mutations of CusB methionines 21, 36, and 38 to isoleucine decreased the tolerance of the cells to copper comparable with the *cusB* deletion, suggesting that these methionines play an essential role in metal resistance.

The periplasmic proteins clearly function in the cell as part of a multimeric protein complex, although it is not known whether the periplasmic protein itself forms a higher order species. To determine the oligomeric state of CusB *in vitro* in the presence and absence of substrate, we performed sedimentation equilibrium analysis. From this technique the molecular mass of the protein species can be determined in a shape-independent manner. Data from three different concentrations of protein, 5, 9, and 14 μM, with and without Ag(I), were fit well with a single ideal species model at all speeds, with residuals in the acceptable range (data for 9 μM protein concentration are shown in Fig. 4, and data for 5 and 14 μM protein concentrations are not shown.). From these experiments, the molecular masses of apo-CusB and CusB-Ag(I) were predicted to be ~43 kDa, consistent with the calculated value of 43.8 kDa. These results indicate that CusB is monomeric in solution, similar to the isolated periplasmic proteins from the HAE family of RND efflux systems (32, 33). Additionally, these data show that the oligomeric state of CusB does not change in the absence and presence of metal.

The structural properties of CusB in the apo- and Ag(I)-bound states were further analyzed using analytical gel filtration chromatography. Elution volumes from a gel filtration column can determine the relative molecular weight of a species as compared with globular calibration proteins. However, unlike sedimentation equilibrium where molecular weight determination is independent of protein shape, analytical gel filtration retention volumes, and in turn the molecular weight calculation, can be significantly affected by the shape of the protein. Based on homology to two periplasmic proteins from the HAE family of RND systems for which structures have been determined (11, 33, 34), CusB is expected to have a nonglobular, elongated structure. Fig. 5 shows the elution profiles of CusB in both the apo- and Ag(I)-loaded forms. As expected, both apo- and metal-bound CusB elute from the column with less volume than expected for a 43-kDa globular protein, which likely reflects an elongated shape. However, there is a marked difference in the elution volumes between apo-CusB and CusB-Ag(I). The apoprotein elutes from the column at a retention volume of 14.1 ml, whereas CusB-Ag(I) elutes at a retention volume of 14.6 ml. As the analytical ultracentrifugation data clearly indicate that apo-CusB and CusB-Ag(I) are monomeric, the change in elution volume is indicative of a conformational change. The decrease in retention volume of CusB-Ag(I) compared with apo-CusB suggests that CusB undergoes a conformational change upon binding silver to a more globular state.

DISCUSSION

We have demonstrated that the periplasmic protein CusB is a metal-binding protein and have identified the three residues that are most likely to play a role in metal coordination. Furthermore, we have shown that defects in metal binding result in a loss of metal resistance *in vivo*, suggesting that CusB metal binding plays an important role in metal resistance in this system. Substrate binding by a periplasmic protein has not been previously demonstrated in an RND efflux system. In two distantly related non-RND tripartite export systems where the inner membrane protein belongs to either the major facilitator superfamily or the ATP-binding cassette superfamily, the periplasmic portions of these systems have been shown to bind substrate (35, 36). However, in RND efflux systems, the only reported substrate-binding site is in the inner membrane protein (37).

Substrate binding by CusB suggests that it could have a direct role in substrate efflux and that it does not simply serve as a passive anchor required to link the inner and the outer membrane components. It is possible that the substrate bound by CusB is subsequently exported from the cell. Studies from several other systems have demonstrated that substrates that originate in the periplasm can be exported. Genetic evidence sug-

gests that in the case of Cu(I) and Ag(I) transport in *E. coli*, the inner membrane P-type ATPase CopA is likely responsible for transport across the inner membrane, and that the CusCFBA system does not serve a redundant function to CopA (38). Thus, the most likely origin of substrate transported by CusCFBA is from the periplasm. Uptake of a metal substrate from the periplasm is supported by studies of the divalent metal export system CzcCBA from *Cupriavidus* (formerly *Ralstonia*) *metallidurans*. In this case an additional system that transports Co(II) from the cytoplasm to the periplasm was absolutely required for CzcCBA function, implying that CzcCBA takes up its substrate from the periplasm (39). In addition, CzcCBA was rendered ineffective in the absence of CadA and ZntA P-type ATPases, which translocate Cd(II) and Zn(II) from the cytoplasm to the periplasm (39). Other systems similarly suggest a periplasmic mode of drug entry (14, 40).

We have demonstrated that substrate binding is linked to a conformational change to a more compact state. Conformational changes in periplasmic proteins from other systems have been proposed previously. Four conformations of AcrA were captured in the asymmetric unit of the AcrA crystal, which differed in the position of the α-helical domain with respect to the lipoyl domain (11). Additionally, using EPR spectroscopy, AcrA was reported to undergo a conformational rearrangement triggered by pH changes (41). Molecular dynamics simulations also suggest inter-domain motions of the periplasmic protein MexA (42). In all these studies, the suggested consequence of the conformational flexibility is in the association of the three components and the opening or closing of the inner and outer membrane proteins of the tripartite complex.

From our studies, we conclude that the periplasmic protein CusB of the CusCFBA complex has a substrate-linked role beyond that of a scaffolding protein bridging the inner and outer membrane components. It is possible that metal binding to CusB induces a conformational change to open the outer membrane protein channel, or CusB may hand off metal to the inner membrane complex for export. In previous studies of RND efflux systems, substrate binding has only been reported for the inner membrane protein. It is possible that in the Cu(I)/Ag(I) efflux system, where a very specific substrate is exported, substrate selection by the periplasmic component could provide the needed specificity.

Acknowledgments—We thank Sylvia Franke for assistance with molecular biology techniques and Dietrich Nies for kindly providing E. coli strain EC950.

REFERENCES

1. Poole, K., and Srikumar, R. (2001) *Curr. Top. Med. Chem.* **1,** 59–71
2. Piddock, L. J. V. (2006) *Nat. Rev. Microbiol.* **4,** 629–636
3. Yang, S., Lopez, C. R., and Zechiedrich, E. L. (2006) *Proc. Natl. Acad. Sci. U. S. A.* **103,** 2386–2391
4. Tseng, T. T., Gratwick, K. S., Kollman, J., Park, D., Nies, D. H., Goffeau, A., and Saier, M. H., Jr. (1999) *J. Mol. Microbiol. Biotechnol.* **1,** 107–125
5. Dinh, T., Paulsen, I. T., and Saier, M. H., Jr. (1994) *J. Bacteriol.* **176,** 3825–3831
6. Poole, K. (2004) *Clin. Microbiol. Infect.* **10,** 12–26
7. Touze, T., Eswaran, J., Bokma, E., Koronakis, E., Hughes, C., and Koronakis, V. (2004) *Mol. Microbiol.* **53,** 697–706
8. Eswaran, J., Koronakis, E., Higgins, M. K., Hughes, C., and Koronakis, V. (2004) *Curr. Opin. Struct. Biol.* **14,** 741–747
9. Zgurskaya, H. I., and Nikaido, H. (2000) *Mol. Microbiol.* **37,** 219–225
10. Franke, S., Grass, G., Rensing, C., and Nies, D. H. (2003) *J. Bacteriol.* **185,** 3804–3812
11. Mikolosko, J., Bobyk, K., Zgurskaya, H. I., and Ghosh, P. (2006) *Structure (Lond.)* **14,** 577–587
12. Lobedanz, S., Bokma, E., Symmons, M. F., Koronakis, E., Hughes, C., and Koronakis, V. (2007) *Proc. Natl. Acad. Sci. U. S. A.* **104,** 4612–4617
13. Augustus, A. M., Celaya, T., Husain, F., Humbard, M., and Misra, R. (2004) *J. Bacteriol.* **186,** 1851–1860
14. Aires, J. R., and Nikaido, H. (2005) *J. Bacteriol.* **187,** 1923–1929
15. Franke, S., Grass, G., and Nies, D. H. (2001) *Microbiology* **147,** 965–972
16. Munson, G. P., Lam, D. L., Outten, F. W., and O'Halloran, T. V. (2000) *J. Bacteriol.* **182,** 5864–5871
17. Outten, F. W., Huffman, D. L., Hale, J. A., and O'Halloran, T. V. (2001) *J. Biol. Chem.* **276,** 30670–30677
18. Solioz, M. (2002) *Biochem. Soc. Trans.* **30,** 688–691
19. Bradford, M. M. (1976) *Anal. Biochem.* **72,** 248–254
20. Jelesarov, I., and Bosshard, H. R. (1999) *J. Mol. Recognit.* **12,** 3–18
21. Kittleson, J. T., Loftin, I. R., Hausrath, A. C., Engelhardt, K. P., Rensing, C., and McEvoy, M. M. (2006) *Biochemistry* **45,** 11096–11102
22. George, G. N. (1990) Stanford Synchrotron Radiation Laboratory, Menlo Park, CA
23. Binsted, N., Gurman, S. J., and Campbell, J. W. (1998) *EXCURVE*, 9.2 Ed., Daresbury Laboratory, Warrington, UK
24. Gurman, S. J., Binsted, N., and Ross, I. (1984) *J. Phys. Chem.* **17,** 143–151
25. Gurman, S. J., Binsted, N., and Ross, I. (1986) *J. Phys. Chem.* **19,** 1845–1861
26. Binsted, N., and Hasnain, S. S. (1996) *J. Synchrotron Radiation* **3,** 185–196
27. Blackburn, N. J., Ralle, M., Hassett, R., and Kosman, D. J. (2000) *Biochemistry* **39,** 2316–2324
28. Laue, T. M., Shah, B. D., Ridgeway, T. M., and Pelletier, S. L. (1992) in *Analytical Ultracentrifugation in Biochemistry and Polymer Science* (Harding, S. R., Rowe, A. J., and Horton, J. C., eds) pp. 90–125, Royal Society of Chemistry, Cambridge, UK
29. McRorie, D. K., and Voelker, P. J. (1993) *Self-associating Systems in the Analytical Ultracentrifuge*, pp. 1–61, Beckman Instruments, Inc., Fullerton, CA
30. Ralle, M., Lutsenko, S., and Blackburn, N. J. (2003) *J. Biol. Chem.* **278,** 23163–23170
31. Pickering, I. J., George, G. N., Dameron, C. T., Kurz, B., Winge, D. R., and Dance, I. G. (1993) *J. Am. Chem. Soc.* **115,** 9498–9505
32. Zgurskaya, H. I., and Nikaido, H. (1999) *J. Mol. Biol.* **285,** 409–420
33. Higgins, M. K., Bokma, E., Koronakis, E., Hughes, C., and Koronakis, V. (2004) *Proc. Natl. Acad. Sci. U. S. A.* **101,** 9994–9999
34. Akama, H., Matsuura, T., Kashiwagi, S., Yoneyama, H., Narita, S. I., Tsukihara, T., Nakagawa, A., and Nakae, T. (2004) *J. Biol. Chem.* **279,** 25939–25942
35. Borges-Walmsley, M. I., Beauchamp, J., Kelly, S. M., Jumel, K., Candlish, D., Harding, S. E., Price, N. C., and Walmsley, A. R. (2003) *J. Biol. Chem.* **278,** 12903–12912
36. Thanabalu, T., Koronakis, E., Hughes, C., and Koronakis, V. (1998) *EMBO J.* **17,** 6487–6496
37. Murakami, S., Nakashima, R., Yamashita, E., Matsumoto, T., and Yamaguchi, A. (2006) *Nature* **443,** 173–179
38. Grass, G., and Rensing, C. (2001) *J. Bacteriol.* **183,** 2145–2147
39. Munkelt, D., Grass, G., and Nies, D. H. (2004) *J. Bacteriol.* **186,** 8036–8043
40. Nikaido, H., Basina, M., Nguyen, V., and Rosenberg, E. Y. (1998) *J. Bacteriol.* **180,** 4686–4692
41. Ip, H., Stratton, K., Zgurskaya, H., and Liu, J. (2003) *J. Biol. Chem.* **278,** 50474–50482
42. Vaccaro, L., Koronakis, V., and Sansom, M. S. P. (2006) *Biophys. J.* **91,** 558–564

Substrate-linked Conformational Change in the Periplasmic Component of a Cu(I)/Ag(I) Efflux System

Ireena Bagai, Wenbo Liu, Christopher Rensing, Ninian J. Blackburn and Megan M. McEvoy

J. Biol. Chem. 2007, 282:35695-35702.
doi: 10.1074/jbc.M703937200 originally published online September 24, 2007
